

Relativistic effects on the Richtmyer-Meshkov instability

F. Mohseni,^{1,*} M. Mendoza,^{1,†} S. Succi,^{2,‡} and H. J. Herrmann^{1,3,§}

¹*ETH Zürich, Computational Physics for Engineering Materials, Institute for Building Materials, Wolfgang-Pauli-Strasse 27, HIT, CH-8093 Zürich (Switzerland)*

²*Istituto per le Applicazioni del Calcolo C.N.R., Via dei Taurini, 19 00185, Rome (Italy), and Freiburg Institute for Advanced Studies, Albertstrasse, 19, D-79104, Freiburg, (Germany)*

³*Departamento de Física, Universidade Federal do Ceará, Campus do Pici, 60455-760 Fortaleza, Ceará, (Brazil)*

(Dated: August 21, 2018)

Theoretical and numerical analysis of the relativistic effects on the Richtmyer-Meshkov (RM) instability reveals new and potentially very useful effects. We find that, in contrast with the non-relativistic case, the growth rate of the RM instability depends strongly on the equation of state of the fluid, opening up the possibility to infer equations of state from experimental observations of the RM instability. As opposed to the non-relativistic case, we also discover that, above a critical value of the fluid velocity, the growth rate of the instability counter-intuitively decreases due to the Lorentz's factor, and vanishes in the ultrarelativistic limit, as the speed of the particles approaches the speed of light. Both effects might prove very useful for leading-edge applications, such as the study of the equation of state of quark-gluon matter, and the design of fast ignition inertial confinement fusion (ICF) schemes. We perform a linear stability analysis to characterize the instability, for an arbitrary equation of state, and implement numerical simulations to study the instability in the non-linear regime, using the equation of state of an ideal gas. Furthermore, based on the numerical results, we propose a general expression that characterizes the long term evolution of the instability.

PACS numbers: 47.75.+f, 47.20.-k, 95.30.Sf, 25.75.-q, 52.57.Kk

The Richtmyer-Meshkov instability is one of the fundamental fluid instabilities, which occurs when a shock wave passes through an interface, separating two fluids with different densities. This instability was theoretically predicted by Richtmyer [1] and experimentally detected by Meshkov [2] in the non-relativistic context. The study of the RM instability is of major importance in several fields, ranging from high energy physics [3] to astrophysics [4], especially wherever shock-wave propagation is involved. In a collapsing core supernova explosion, the generated shock wave propagates outwards through a hydrogen-helium interface. Observations have shown that the outer regions of the supernovae are more uniformly mixed than expected, as a consequence of the RM instability [4]. Therefore, the study of the relativistic effects, from the theoretical point of view, can contribute to a deeper understanding of this phenomenon. On a very different front, it has been recently discovered that quark-gluon plasma (QGP) behaves as a nearly perfect fluid [5–7], where shock waves have been theoretically predicted [8] and experimentally observed [9, 10]. However, the equation of state of this extreme state of matter is still under debate [11–13], and therefore, developing new strategies to determine its form represents a very important subject of research [14]. The existence of relativistic shock-waves can lead to the appearance of the RM instability. In this Letter, we show that the RM instability can also be used for this purpose, since, in contrast to the non-relativistic case, the growth rate of the instability depends explicitly on the equation of state. As a result, experimental information from the RM instability can

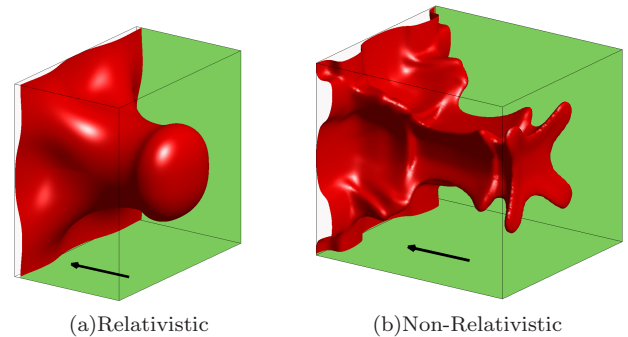


FIG. 1. Snapshots of the interface in the three dimensional shock tube Richtmyer-Meshkov instability at time $t = 570$. The pre-shock density ratio is 28 and the Mach number is 2.4. Arrows show the direction of the shock wave.

be used to distinguish between different theoretical models [15, 16]. The RM instability also plays a significant role in inertial confinement fusion (ICF) [3], which has recently captured significant attention as an alternative source of energy [17]. Like most instabilities, the RM and Rayleigh-Taylor instabilities represent one major cause of performance degradation in energy applications [18, 19]. Fast ignition ICF approach uses a relativistic beam of electrons to heat the compressed fuel, where relativistic fluid dynamic models can describe the plasma-electron interactions [20, 21]. Since there is not any theoretical description for the RM instability in the relativistic context, the design of better schemes becomes more difficult. Thus, the results in this letter can be used to enhance

the performance of the fast ignition ICF schemes (see Fig.1 for a comparison between the relativistic and non-relativistic RM instabilities, where we can appreciate the damping of the instability due to the relativistic effects), as for instance, the fact that above a critical value of the fluid velocity the RM instability presents a damping due to the Lorentz's factor.

In the non-relativistic context, the RM instability has been investigated extensively [1, 22–25]. However, to the best of our knowledge, a systematic study of the RM instability in the relativistic regime is still lacking. In this Letter, we first perform a linear stability analysis of the relativistic RM instability and derive a theoretical asymptotic expression for the growth rate of the perturbation amplitude. In order to verify the theoretical results and to obtain a general expression for the amplitude in the non-linear regime, we perform numerical simulations of the relativistic RM instability. To this purpose, the recently introduced relativistic lattice Boltzmann model for high velocities [26–29] was extended to deal with the ideal gas equation of state. In order to single out the relativistic effects, we also provide comparisons between the relativistic and non-relativistic cases, and present a study of the growth rate of the instability for different equations of state.

Let us start by considering the growth of irregularities - in particular sinusoidal corrugations - at the interface between two fluids in the relativistic RM instability, i.e., when a relativistic shock wave passes through the interface. In analogy to the non-relativistic case [1], we first approach the problem by studying the Rayleigh-Taylor instability, which takes place at the interface between two fluids at different densities, whenever one of the two fluids accelerates into the other, and later we replace the constant acceleration by an impulsive one representing the shock wave.

The conservation equations of relativistic fluid dynamics are $\partial_\alpha T^{\alpha\beta} = G^\beta$, and $\partial_\alpha N^\alpha = 0$, where $T^{\alpha\beta}$ is the energy-momentum tensor, N^α is the particle four-flow and G^β is the force density. For an ideal (inviscid) fluid we have $T^{\alpha\beta} = (\epsilon + p)U^\alpha U^\beta / c^2 - p\eta^{\alpha\beta}$, and $N^\alpha = nU^\alpha$, where p is the hydrostatic pressure, ϵ the energy density (including the rest mass energy), c is the speed of light and $\eta^{\alpha\beta}$ is the Minkowski metric tensor with the signature $(+, -, -, -)$. The macroscopic four-velocity is $(U^\mu) = (c, \vec{u})\gamma(u)$, with \vec{u} being the three-dimensional velocity and $\gamma(u) = 1/\sqrt{1 - u^2/c^2}$ the Lorentz's factor. The relativistic force density can be defined as $G^\alpha \equiv (\vec{F} \cdot \vec{u}\gamma(u)/c, \vec{F}\gamma(u))$, where \vec{F} is the three-dimensional force density vector [30], and n is the number of particles density. Note that the Einstein summation convention is assumed here and throughout this paper. For the sake of simplicity, natural units i.e., $c = k_B = m = 1$ are assumed hereafter. For the Rayleigh-Taylor instability, we consider $\vec{F} = (\epsilon + p)\vec{g}$, where \vec{g} is the acceleration.

To calculate the amplitude growth rate of the distur-

bance at the interface, we perform a linear stability analysis and without loss of generality, we deal with this problem in two dimensions. Thus, small perturbations are assumed for the velocity along x and y directions, i.e., δu and δv , and the physical variables, such as the density and pressure, i.e., δp and δn . For a single mode disturbance, we write $A(x, y, t) = A_k(x) \exp(iky + \omega t)$, where A stands for δu , δv , δp and δn , as well as the amplitude of the perturbation h . Here $k = 2\pi/\lambda$ is the wave number, λ is the initial perturbation wavelength and ω is the wave frequency of the perturbations.

We suppose that at $t = 0$ the interface is located at $x = 0$, and the only non-zero component of \vec{g} is in x direction, i.e., g . To include the condition of incompressibility, and considering the fact that second order terms play no role in the linear stability analysis, the continuity equation simplifies to $\vec{\nabla} \cdot \vec{u} = 0$. Assuming that pressure and density are functions of x only, we substitute the perturbed quantities in the conservation equations and the incompressibility condition. Dropping the nonlinear terms and considering initial equilibrium at the interface, i.e., $\partial p/\partial t = 0$, we obtain a system of linear differential equations.

Solving these equations, and taking $g/k \ll 1$, we find the following dispersion relation, $\omega^2 = (n_2 - n_1)gk/(2p + \epsilon_1 + \epsilon_2)\gamma$, where ϵ_1 and ϵ_2 are the energy densities at both sides of the interface. In the non-relativistic limit $\gamma \sim 1$, using the equation of state of an ideal gas [31], i.e., $\epsilon + p = (\frac{1}{\Gamma-1} + 1)p + n$, and considering $k_B T \ll mc^2$ (so that pressure can be ignored with respect to the density), we get the well known dispersion relation of the non-relativistic Rayleigh-Taylor instability. Here Γ is the adiabatic index, i.e., specific heat at constant pressure divided by specific heat at constant volume (see Supplementary Material [32]). Moreover, by using the equation of state of an ideal gas with $\Gamma = 4/3$ and removing the Lorentz's factor, we obtain the relation for the Rayleigh-Taylor instability for the ultra-relativistic case [33]. Hence, the amplitude of the perturbed interface grows according to

$$\frac{\partial^2 h(t)}{\partial t^2} = \omega^2 h(t). \quad (1)$$

In order to find a relation for the relativistic RM instability, we replace the constant acceleration by an impulsive acceleration, representing the shock wave. Let Δu be the increment of velocity due to this impulsive acceleration, we have $g(t) = \Delta u \delta(t)$, where $\delta(t)$ is the Dirac delta function. Integrating Eq.(1) and using the fact that $\int g(t)dt = \Delta u$, we obtain the asymptotic relation for the growth rate of the perturbation amplitude in the linear regime of the relativistic RM instability:

$$v_f \equiv \frac{\partial h(t)}{\partial t} = \frac{(n_2 - n_1)kh_0\Delta u}{\gamma(2p + \epsilon_2 + \epsilon_1)}. \quad (2)$$

Here, h_0 is the initial amplitude of the perturbation.

Note that this is a general expression which holds for any equation of the state $\epsilon = \epsilon(T)$ and $p = p(T)$, where T is the fluid temperature. This shows that, unlike its non-relativistic counterpart, the growth rate of the amplitude for the relativistic RM instability depends on the equation of state.

In the RM instability, the light fluid penetrates the heavy one, generating bubbles and the heavy fluid penetrates the light one, giving rise to spikes. The perturbation amplitude, $h(t)$, is calculated by measuring the distance between the tips of the spike and the bubble divided by two. Note that the linear assumption is well justified only as long as the interface amplitude is small, i.e., $h/\lambda < 0.1$ [34] and nonlinear effects become important when the amplitude becomes larger.

One can immediately notice from Eq.(2) that relativistic effects decrease the amplitude growth rate compared to the non-relativistic RM instability, due to the Lorentz's factor, $\gamma > 1$, as well as to the contribution of the pressure to the inertia of the relativistic fluid, which becomes relevant at high temperatures. This argument is in line with previous observations in [35], which show a delay in the onset of pre-turbulence of relativistic electronic micro-jets in graphene.

Note that, in the presence of the shock wave, Eq.(2) permits to find the asymptotic linear growth rate of the amplitude, using the post-shock values of n_1 , n_2 and h_0 , Δu and p being the velocity jump and pressure at the interface.

To find a general relation for the amplitude in the non-linear regime, we perform numerical investigations of the relativistic RM instability, using the lattice Boltzmann model for high velocities recently proposed in [26] (for more details see Supplementary Material [32]). Note that using the relativistic Boltzmann model leads to viscous hydrodynamics. However, it has been shown that viscosity has a negligible effect on the perturbation amplitude in the non-relativistic shock tube RM instability [36, 37], so that we expect a similar behavior in relativistic hydrodynamics. For the two-dimensional simulation of the shock tube RM instability, a domain of 200×1200 lattice cells is considered. Since we use dimensionless numbers to characterize the RM instability, we refer to numerical units throughout this Letter. For all the simulations considered here, a shock wave with the velocity $\beta = |\vec{u}|/c = 0.94$, traveling from right to left, is passing through a sinusoidal perturbation in the density located at $x_p = 1000$ cells. The initial position of the shock wave is at $x_s = 1100$ cells. The single mode sinusoidal perturbation at the interface is: $x = x_p + a \sin(\frac{\pi}{2} + \frac{2\pi}{\lambda}y)$, where a is the pre-shock amplitude of the interface and λ is the width of the domain. Note that, hereafter the subscripts R , M , and L refer to the right hand side of the shock, the region between the shock and the initial perturbation, and the left hand side of the perturbation, respectively. The densities at the two sides of the perturbation are dif-

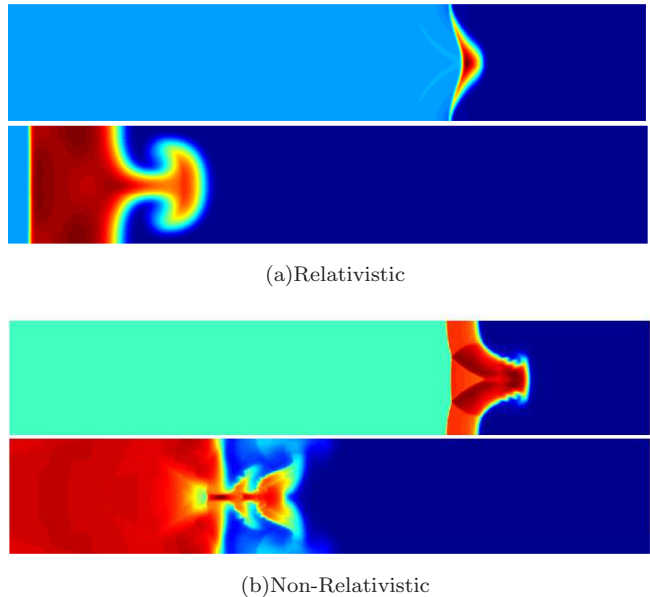


FIG. 2. Snapshots of the density field in the two dimensional shock tube Richtmyer-Meshkov instability for (a) relativistic and (b) non-relativistic cases at different times. For both cases, from top to bottom, snapshots corresponds to the times $t = 180$ and $t = 1260$, respectively. Here, $n_L/n_M = 28$ and Mach number is 2.4. Blue and red colors denote low and high densities, respectively. Here, time represents the number of time steps multiplied by $\delta t/\delta x = 0.15$.

ferent, and the pressure is forced to be constant across the perturbation, i.e., $p_M = p_R$, by choosing appropriate values of the temperature. For simplicity, the simulations have been performed assuming the equation of state of an ideal gas for various pre-shock density ratios n_L/n_M and various values of the relativistic Mach number of the shock wave $Ma_r = u_s \gamma(u_s)/c_s \gamma(c_s)$, where the velocity of the shock u_s and the sound velocity c_s are defined as [31, 38]

$$u_s^2 = \frac{(p_R - p_M)(\epsilon_R + p_M)}{(\epsilon_M + p_R)(\epsilon_R - \epsilon_M)}, \quad c_s^2 = \frac{\Gamma(\Gamma - 1) \frac{p_M}{n_M}}{\Gamma \frac{p_M}{n_M} + \Gamma - 1}. \quad (3)$$

The values of initial densities and pressures are calculated in such a way as to obtain the desired values of n_L/n_M and Ma_r , while the velocity of the shock is fixed. For more details, see Supplementary Material [32].

Fig. 2(a) shows the density field and the evolution of the bubble and the spike for the case $n_L/n_M = 28$, $Ma_r = 2.4$ and $a = 32$ at different times, after the shock wave has passed through the initial perturbation. Finally, the spike forms the characteristic mushroom shape of the instability. It is worth mentioning that the passage of the shock wave through the heavy fluid causes an increase in its density, due to the compression, which is well visible in Fig. 2.

For the purpose of comparison, we have also performed a numerical simulation for the non-relativistic RM at the

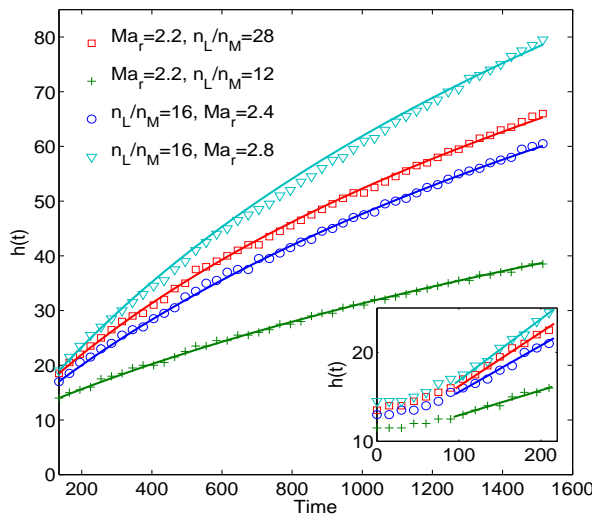


FIG. 3. Results of the numerical simulation $h(t)$ versus time for different Ma_r and density ratios in the nonlinear regime. Solid lines are the resulting $h(t)$, using the proposed relation, Eq.(4). In the inset, the results for linear regime are presented and the solid lines show the asymptotic theoretical growth rate, Eq.(2).

same density ratio and Mach number as in Fig. 2(a), i.e., $n_L/n_M = 28$ and $Ma = 2.4$. The results are presented in Fig. 2(b). Here, in order to draw an accurate comparison between the two cases, and regarding the fact that we are simulating viscous hydrodynamics, the Reynolds number should also be the same for both cases. Thus, following Ref.[39], we define the relativistic Reynolds number for the shock tube relativistic RM instability as $Re_r = (\epsilon + p)u_s\gamma(u_s)\lambda/\eta$, where η is the shear viscosity. For the non-relativistic numerical simulations, we have used the model proposed in Ref.[40]. Fig. 2(b) shows that, in the non-relativistic RM, the amplitude of the perturbation grows much faster at early times, leading to a faster development and more complex structures of the instability at later times. In fact, this agrees with our analytical results, Eq.(2), where we argued that relativistic effects lead to a damping of the instability. This can be also seen in Fig. 1, where the results of the simulation for the 3D shock tube RM instability with square cross section is presented, with $n_L/n_M = 28$ and the $Ma_r = Ma = 2.4$. The 3D simulation was performed with the same parameters as before and using a lattice size of $200 \times 200 \times 1200$ cells.

Since Eq.(2) predicts an asymptotic growth rate of the amplitude in the linear regime, we are now interested in a general relation for the growth rate of the amplitude of the instability in the nonlinear regime. For the shock tube RM instability and for fixed adiabatic index and wave number and in the absence of surface tension, the amplitude depends on density ratio and Mach number.

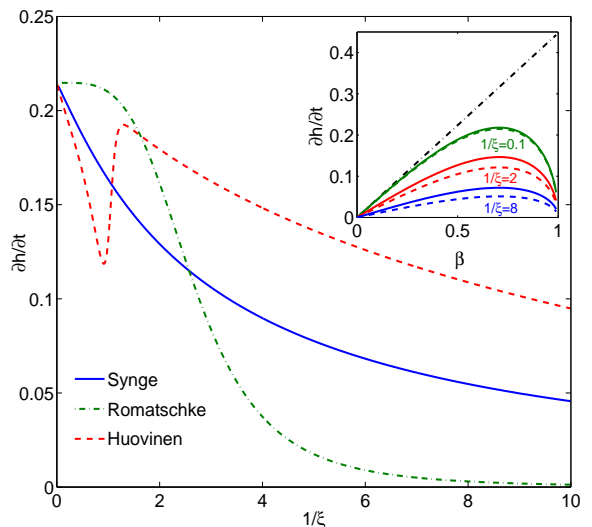


FIG. 4. Perturbation growth rate in the linear regime calculated from Eq.(2) as a function of temperature for different equations of state proposed in Refs. [41], [15] and [16]. In the inset, we see the effect of increasing $\beta = \Delta u/c$ on the perturbation growth rate in the linear regime (using the ideal gas equation of state: solid lines for $\Gamma = 5/3$ and dashed lines for $\Gamma = 4/3$), for different temperatures, comparing with the non-relativistic RM instability (dashed-dotted line).

Therefore, several simulations have been performed for different density ratios and relativistic Mach numbers, i.e., $8 \leq n_L/n_M \leq 28$ and $2 \leq Ma_r \leq 3$, when $a = 16$. Fig. 3 shows the numerical results of $h(t)$ for different values of Ma_r and density ratios in the nonlinear regime. By increasing Ma_r , as well as the density ratio, the amplitude grows faster. Note that v_f can be used as the initial growth rate of the nonlinear regime. In order to describe the effect of the nonlinearity on the growth rate, we propose the following relation (see Fig. 3),

$$\frac{\partial h(t)}{\partial t} = \frac{v_f}{1 + a_1 \left(\frac{v_f}{n_M}\right)^{1/2} Ma_r t}, \quad (4)$$

where $a_1 = 9.033 \times 10^{-5}$ is a constant value. Note that this constant is independent of the Mach number and the density ratio, and therefore we can assume that this is a universal constant characterizing the instability. In the inset of Fig. 3, the results of $h(t)$ for the linear regime are presented, where the slope of the solid lines represents the theoretical growth rate, Eq.(2). As expected, at early times, the compressibility effects decrease the growth rate, but at later times, when the compressibility effects are weaker, very good agreement is found between the theoretical, Eq. (2) and numerical growth rates.

In order to explore the consequences of the relativistic effects, we plot the asymptotic linear growth rate of the instability, Eq.(2) as a function of the temperature, for different equations of state (see Fig. 4). Here, we compare

the equation of state for an ideal relativistic gas developed by Synge [41], the non-ideal equation of state for QGP proposed by Romatschke [15], and the equation of state for strongly interacting matter in relativistic heavy ion collision (with a phase transition) proposed by Huovinen [16]. We have defined the dimensionless parameter $\xi = mc^2/k_B T$ and the following parameters are considered: $h_0 = 20$, $k = 0.025$, $\Delta u = 0.6$, and the post-shock density ratio is 18. Fig. 4 shows that the perturbation growth rate strongly depends on the equation of state, and therefore, the RM instability can be used to check the validity of a proposed equation of state. In the inset of Fig. 4, the linear growth rate of the amplitude versus the velocity, $\beta = \Delta u/c$, for the ideal gas equation of state, is compared with the respective relation for the non-relativistic RM instability, at different temperatures. Note that for low velocities and low temperatures, both relations agree, but by further increasing β and/or the temperature, the perturbation amplitude decreases as compared to the non-relativistic case. Note that the value of $\beta = 1/\sqrt{2}$ optimizes the growth of the perturbation in the relativistic RM instability and for the case of massless particles, $\beta = 1$, the growth rate of the instability vanishes. Additionally, each relativistic result in the inset of Fig. 4 is presented for two cases, $\Gamma = 5/3$ and $\Gamma = 4/3$, and, as expected, the results with $\Gamma = 5/3$ are closer to the non-relativistic ones.

Summarizing, we have shown that the RM instability can be exploited to distinguish between different equations of state, by measuring the growth rate of the instability. This result can be used as a method to determine the equation of state of QGP, which is still under debate. In addition, by increasing the jump velocity across the interface above a critical value, the growth of the instability decreases and eventually goes to zero for $\beta = 1$. This is an unexpected result because one would expect that for higher velocities the fluid should become more unstable. This effect can be exploited for improving the design of fast ICF schemes, where damping of the instability would prove beneficial to the overall efficiency of the process. We have also proposed a long-term relation for the evolution of the interface amplitude for different values of the density ratio and relativistic Mach number. To study analytically the relativistic effects, we have developed a linear impulsive model, based on the linear instability analysis, to predict the asymptotic amplitude growth rate of the interface in the linear regime. Developing new theoretical results for compressible cases and non-linear regimes, and investigating other types of equation of state, makes a very interesting subject for further research.

We acknowledge financial support from the European Research Council (ERC) Advanced Grant 319968-FlowCCS. The authors are also grateful for the financial support of the Eidgenössische Technische Hochschule Zürich (ETHZ) under Grant No. 0611-1.

-
- * mohsenif@ethz.ch
† mmendoza@ethz.ch
‡ succi@iac.cnr.it
§ hjherrmann@ethz.ch
- [1] R. D. Richtmyer, *Commun. Pure Appl. Math.* **13**, 297 (1960).
 - [2] E. Meshkov, *Fluid Dyn.* **4**, 101 (1969).
 - [3] V. Goncharov, *Phys. Rev. Lett.* **82**, 2091 (1999).
 - [4] D. Arnett, *Astrophys. J. Supp. Ser.* **127**, 213 (2000).
 - [5] S. S. Adler, S. Afanasiev, C. Aidala, N. Ajitanand, Y. Akiba, J. Alexander, R. Amirkas, L. Aphecetche, S. Aronson, R. Averbeck, *et al.* (PHENIX Collaboration), *Phys. Rev. Lett.* **91**, 182301 (2003).
 - [6] J. Adams, C. Adler, M. Aggarwal, Z. Ahammed, J. Amonett, B. Anderson, M. Anderson, D. Arkhipkin, G. Averichev, S. Badyal, *et al.* (STAR Collaboration), *Phys. Rev. Lett.* **92**, 052302 (2004).
 - [7] B. Back, M. Baker, M. Ballintijn, D. Barton, R. Betts, A. Bickley, R. Bindel, A. Budzanowski, W. Busza, A. Carroll, *et al.* (PHOBOS Collaboration), *Phys. Rev. C* **72**, 051901 (2005).
 - [8] W. Scheid, H. Müller, and W. Greiner, *Phys. Rev. Lett.* **32**, 741 (1974).
 - [9] H. H. Gutbrod, A. M. Poskanzer, and H. G. Ritter, *Rep. Prog. Phys.* **52**, 1267 (1989).
 - [10] H. H. Gutbrod, K. H. Kampert, B. Kolb, A. M. Poskanzer, H. G. Ritter, R. Schicker, and H. R. Schmidt, *Phys. Rev. C* **42**, 640 (1990).
 - [11] D. Fogaça, L. Ferreira Filho, and F. Navarra, *Phys. Rev. C* **81**, 055211 (2010).
 - [12] P. N. Meisinger, T. R. Miller, and M. C. Ogilvie, *Phys. Rev. D* **65**, 034009 (2002).
 - [13] V. Begun, M. Gorenstein, and O. Mogilevsky, *Int. J. Mod. Phys. E* **20**, 1805 (2011).
 - [14] I. Bouras, E. Molnar, H. Niemi, Z. Xu, A. El, O. Fochler, C. Greiner, and D. Rischke, *Phys. rev. Lett.* **103**, 032301 (2009).
 - [15] P. Romatschke, *Phys. Rev. D* **85**, 065012 (2012).
 - [16] P. Huovinen, *Nucl. Phys. A* **761**, 296 (2005).
 - [17] E. Hand, *Nature* **483**, 133 (2012).
 - [18] D. Wilson, C. Cranfill, C. Christensen, R. Forster, R. PETERSON, N. Hoffman, G. Pollak, C. Li, F. Séguin, J. Frenje, *et al.*, *Phys. Plasmas* **11**, 2723 (2004).
 - [19] M. Ottaviani, F. Romanelli, R. Benzi, M. Briscolini, P. Santangelo, and S. Succi, *Physics of Fluids B: Plasma Physics* **2**, 67 (1990).
 - [20] S. Atzeni, A. Schiavi, F. Califano, F. Cattani, F. Cornolti, D. Del Sarto, T. Liseykina, A. Macchi, and F. Pegoraro, *Comput. phys. commun.* **169**, 153 (2005).
 - [21] S. Atzeni, A. Schiavi, and J. Davies, *Plasma Phys. Contr. F.* **51**, 015016 (2009).
 - [22] J. G. Wouchuk and K. Nishihara, *Phys. Plasmas* **3**, 3761 (1996).
 - [23] J. Wouchuk, *Phys. Rev. E* **63**, 056303 (2001).
 - [24] M. Vandenboomgaerde, C. Mügler, and S. Gauthier, *Phys. Rev. E* **58**, 1874 (1998).
 - [25] A. D. Kotelnikov, J. Ray, and N. J. Zabusky, *Phys. Fluids* **12**, 3245 (2000).
 - [26] F. Mohseni, M. Mendoza, S. Succi, and H. J. Herrmann, *Phys. Rev. D* **87**, 083003 (2013).
 - [27] M. Mendoza, B. Boghosian, H. Herrmann, and S. Succi,

- Phys. Rev. Lett. **105**, 014502 (2010).
- [28] D. Hupp, M. Mendoza, I. Bouras, S. Succi, and H. J. Herrmann, Phys. Rev. D **84**, 125015 (2011).
- [29] M. Mendoza, I. Karlin, S. Succi, and H. J. Herrmann, Phys. Rev. D **87**, 065027 (2013).
- [30] C. Cercignani and G. Kremer, *The Relativistic Boltzmann Equation: Theory and Applications* (Birkhauser, Boston; Basel; Berlin, 2002).
- [31] D. Ryu, I. Chattopadhyay, and E. Choi, Astrophys. J. Supp. Ser. **166**, 410 (2006).
- [32] See Supplementary Material at.
- [33] A. Allen and P. Hughes, Mon. Not. R. Astron. Soc. **208**, 609 (1984).
- [34] M. Brouillette, Annu. Rev. Fluid Mech. **34**, 445 (2002).
- [35] M. Mendoza, H. Herrmann, and S. Succi, Phys. Rev. Lett. **106**, 156601 (2011).
- [36] P. Carlès and S. Popinet, Eur. J. Mech. B-Fluid **21**, 511 (2002).
- [37] M. Jones and J. Jacobs, Phys. Fluids **9**, 3078 (1997).
- [38] D. H. Rischke, S. Bernard, and J. A. Maruhn, Nucl. Phys. A **595**, 346 (1995).
- [39] M. Müller, J. Schmalian, and L. Fritz, Phys. Rev. Lett. **103**, 025301 (2009).
- [40] Q. Li, Y. He, Y. Wang, and W. Tao, Phys. Rev. E **76**, 056705 (2007).
- [41] J. L. Synge, *The relativistic gas* (North-Holland Amsterdam, 1957).